Volume 1 | Number 1 | Jan 2013 | Pages 1–100

ChemComm

Chemical Communications
www.rsc.org/chemcomm

ROYAL SOCIETY OF CHEMISTRY

This is an *Accepted Manuscript*, which has been through the Royal Society of Chemistry peer review process and has been accepted for publication.

Accepted Manuscripts are published online shortly after acceptance, before technical editing, formatting and proof reading. Using this free service, authors can make their results available to the community, in citable form, before we publish the edited article. We will replace this *Accepted Manuscript* with the edited and formatted *Advance Article* as soon as it is available.

You can find more information about *Accepted Manuscripts* in the **Information for Authors**.

Please note that technical editing may introduce minor changes to the text and/or graphics, which may alter content. The journal's standard **Terms & Conditions** and the **Ethical guidelines** still apply. In no event shall the Royal Society of Chemistry be held responsible for any errors or omissions in this *Accepted Manuscript* or any consequences arising from the use of any information it contains.

Fluorescent Detection of RDX within DHPA-Containing Metal-Organic Polyhedra

Liang Zhao, Yulu Chu, Cheng He and Chunying Duan*

By incorporating the dihydropyridine amido group (DHPA) into the rationally designed ligand systems, metal-organic molecular polyhedra were achieved *via* self-assembly for the luminescent sensing of high explosive RDX with the limit of
10 **the detection lower to 1 *ppb* in solution.**

Detecting hidden explosive devices in minefield remediation,[1] crime scene investigations[2] and counter-terrorism applications such as personnel or baggage screening, facility protection, and cargo screening[3] is a pressing concern. The need for ultratrace
15 detection of the commonly used powerful explosives having low-volatility has resulted in an intense interest in fluorescence methods. And numerous optical[4,5] or electrochemical sensors[6,7] for nitroaromatic compounds were developed recently. While cyclotrimethylene trinitramine (RDX) was more powerful than
20 TNT, few high sensitivity RDX probes that exhibits satisfactory properties have been reported, due to that RDX is nonaromatic, it exhibits a three-dimensional flexible structure and just contains one kind of recognition unit (nitramine). Though modifying the reduced nicotinamide adenine dinucleotide (NADH) analogue as
25 reducing agent, metal-organic complexes[8] and CdSe/ZnS QDs[9] have been created for the fluorescent detection of RDX. It is thus hypothesized that the development of three dimensional capsules with appropriate sizes and NADH analogue as suitable triggers represents a powerful strategy to creat RDX sensors with high
30 selectivity and sensitivity.

Metal-organic polyhedra, discrete molecular architectures that constructed through the coordination of metal ions and organic linkers, have attracted considerable attention for their potential for a variety of applications due to their high symmetry, stability
35 and rich chemical/physical properties.[10-14] The architectures that generate well-defined cavities with gated pores provide specific inner environments for the selective uptake and bonding of guest molecules and the catalysis of their reactions.[15] By incorporating N_2O chelators within the ligand backbone, series of metal-organic
40 polyhedra and cyclohelicates constructed have been acted as efficient chemosensors for the selective and sensitive detection of guest molecules with different size, shape and interaction handles. As dihydropyridine amido group (DHPA) is described as the key structure in NADH models[16] and plays an important part in the
45 electron transfer process, herein, we reported the assembly of Ce–**ZPS** and Zn–**ZPT** (See Scheme S1 in the supporting information) metal-organic polyhedra through combining DHPA group into

the rationally designed ligand systems. We envisioned that these capsules would be promising chemosensors for RDX. The well
50 positioned DHPA would provide appropriate matches for polar groups to address the structural diversity of RDX and that the difficulty of selectively recognizing flexible conformations of RDX could be overcome. And these oxidized DHPA fragments possibly exhibited obviously emissions to transform these
55 selective recognition information into measurable luminescent signals. Experimental results suggested that metal-organic octahedron Zn–**ZPT** can function as enzyme-like pockets to encapsulate the explosive RDX molecule and prompt the photoreaction with **DHPA** group in a *ca* 27 fold luminescent
60 enhancement with the limit of detection was improved to 1 ppb.
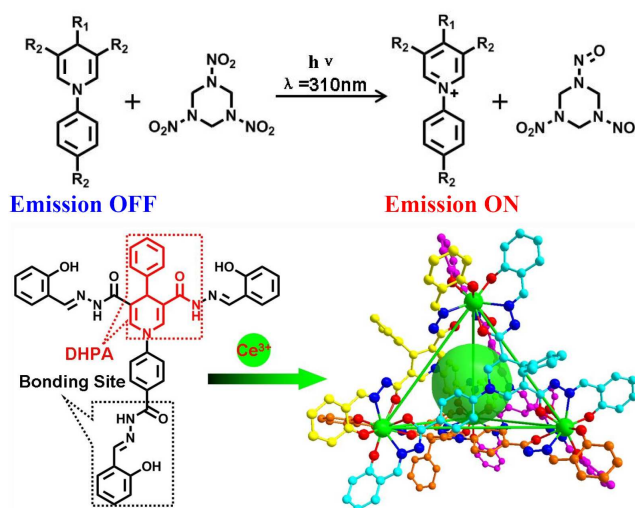
Fig. 1 The constitute/constructional fragments of Ce–**ZPS**. H atoms and solvent molecules are omitted for clarity. The metal, oxygen and nitrogen
65 atoms are drawn in green, red and blue respectively. The carbon atoms are drawn in other colours. Selected bond distances (Å): Ce–O_{phenol} 2.20, Ce–$O_{carbonyl}$ 2.44, Ce–N 2.65.

Ligand H_6**ZPS** was synthesized from salicylaldehyde with 1-(4-(hydrazinecarbonyl)phenyl)-4-phenyl-1,4-dihydropyridine-5-
70 dicarbohydrazide in an ethanol solution and characterized by elemental analysis and spectroscopic methods. Evaporating a DMF solution of H_6**ZPS** containing $Ce(NO_3)_3 \cdot 6H_2O$ generated Ce–**ZPS**, in a high yield (57%). Single-crystal X-ray structural analysis confirmed the formation of a $Ce_4(H_2$**ZPS**$)_4$ tetrahedron in

a crystallographic C_3 symmetry in the solid state (Fig. 1).[17] The tetrahedron comprised four vertical metal centers and four deprotonated H$_2$**ZPS** ligands. Each cerium ion was chelated by three tridentate chelating groups from three different ligands to

5 form a ternate coronary trigonal prism coordination geometry. The four pseudo-C_3 symmetric ligands positioned individually on the four triangle faces of the tetrahedron defined by four metal ions. The Ce···Ce separation was ~13.57 Å, the inner volume of the tetrahedron is about 350 Å^3. The rhombic window of the

10 tetrahedron had a size of 6.8 × 6.5 Å^2, potentially allowing the ingress and egress of small molecules *i.e.* RDX. The benzene ring of DHPA positioned outside of the tetrahedron and its active site positioned interior of cavity. These DHPA moieties thus provided geometric, coordinative and functional properties to the cage-like

15 capsule, ensuring the size and shape selectivity for these host-guest complexation bahaviour. The C−N (DHPA) distance of 1.39 Å is formal single bond, indicating reduction state of the ligand. The C−O and C−N distances within the ligands of 1.26 Å and 1.32 Å, respectively, were intermediate between formal

20 single and double bonds, indicating the extensive delocalization over the entire molecular skeleton.[18] Such a conjugated system is benefical the signalling transduction within the ligand backbone and potentially enhancing the fluorescence response under the interaction with guests.

25 ESI-MS of Ce−**ZPS** in DMF/CH$_3$CN solution exhibited intense peaks at m/z = 1710.24, 1741.73 and 1773.23 with the isotopic distribution patterns separated by 0.50 Da, assignable to the [Ce$_4$(H$_2$**ZPS**)$_2$(H**ZPS**)$_2$]$^{2-}$, [Ce$_4$(H$_2$**ZPS**)$_2$(H**ZPS**)$_2$·2CH$_3$OH]$^{2-}$ and [Ce$_4$(H$_2$**ZPS**)$_2$(H**ZPS**)$_2$·4CH$_3$OH]$^{2-}$, respectively, indicating the

30 successful assembly of a Ce-based M$_4$L$_4$ tetrahedron. Upon the addition of RDX, ESI−MS exhibited a new peak at m/z = 1821.26. An exact comparison of this peak with the simulation results obtained on the basis of natural isotopic abundances revealed the assignment of the peak to the species [Ce$_4$(H$_2$**ZPS**)$_2$(H**ZPS**)$_2$ ⊃

35 RDX]$^{2-}$, demonstrating a 1:1 stoichiometric inclusion behavior. These results suggested that the cavity of Ce−**ZPS** tetrahedron could encapsulate RDX directly, in which the encapsulated RDX reacted with DHPA efficiently to form highly luminescent active species for the experimental detection.
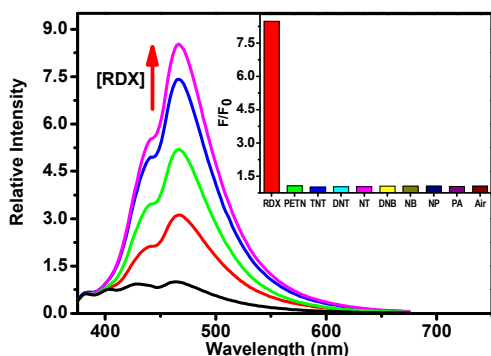
40 **Figure 2** The time-dependent fluorescence growth of Ce−**ZPS** (10 μM) in DMF solution upon addition of the RDX (1 μM) after irradiation with 310 nm light. Spectra were recorded at time intervals of 1 min. The inset shows the fluorescence responses of Ce−**ZPS** towards RDX over various

45 explosives with the emission intensity at 465 nm after a 5 min irradiation (excitation at 350nm).

Compound Ce−**ZPS** (10 μM) exhibited an absorption band centered at about 390 nm in DMF solvent (log ε = 5.22), assignable to the absorptions endemic to the deprotonated phenol

50 groups.[19] When exciting at 350 nm, the solution of Ce−**ZPS** (10 μM) gave an initially weak emission. The addition of the RDX (1 μM) caused a *ca* 8 fold luminescent enhancement after a 5 min irradiation with 310 nm light at 298 K (Fig. 2). The addition of other explosives such as pentaerythritol tetranitrate (PETN),

55 2,4,6-trinitrotoluene (TNT), 2,6-dinitrotoluene (DNT), 2-nitro-toluene (NT), 1,4-dinitrobenzene (DNB), nitrobenzene (NB), 4-nitrophenol (NP) and picric acid (PA) did not cause any significant luminescence variation. The competition experiments of Ce−**ZPS** (10 μM) in the same solution revealed that the

60 fluorescence responses of RDX (1 μM) were unaffected in the presence of other explosives (up to 10 μM), demonstrating the high selectivity of the Ce−**ZPS** toward RDX over other nitramine explosives. Under optimized conditions, with the concentration of Ce−**ZPS** fixed at 5 μM, the fluorescence intensity of the Ce−**ZPS**

65 solution is nearly proportional to the RDX concentration. And the addition of 10 ppb caused about 50 % luminescent enhancement of the solution. It is postulated that the intensity enhancement was contributed to the formation of NAD$^+$ analogue, whereas the selectivity and the sensitivity were resonable attributed to the

70 encapsulation of the RDX within the cavity of the tetrahedron to enforce the proximity between RDX and the reducing site of DHPA, giving a more quickly and sensitivity response towards RDX. To the best of our knowledgement, Ce−**ZPS** represents the first example of the metal-organic polyhedral chemosensors for

75 explosive detection in solution.
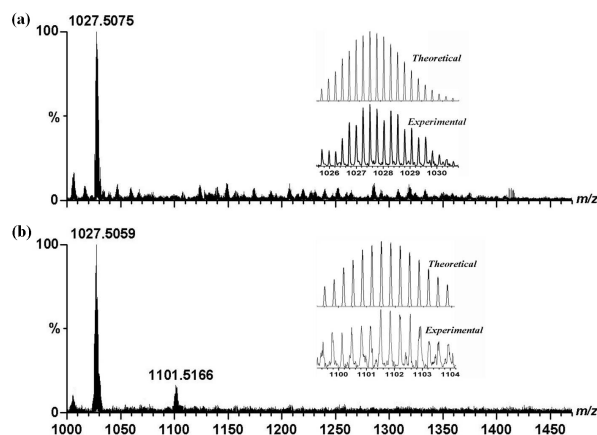
Fig. 3 ESI-MS of (a) Zn−**ZPT** (0.1 mM) and (b) Zn−**ZPT** (0.1 mM) upon addition of 1 equiv of RDX without illumination in DMF/CH$_3$CN solution. Inserts exhibit the measured and simulated isotopic patterns at 1027.51

80 (Top picture) and 1101.52 (Bottom one), respectively

As the N$_2$O chelator and the DHPA reductive triggers were robust enough, our fabricating strategy could be extended to other werner-type capsules composed of transition metal ions. Ligand H$_3$**ZPT** was obtained by the similar Schiff based formation

85 reaction using 2-pyridyl aldehyde and the malonohydrazide in ethanol solution. The metal-organic octahedron was constructed using the d^{10} electron configuration zinc ions and ligand H$_3$**ZPT** through the same strategy.[20] EA and ^{1}H NMR suggested the formation of new compound in the solution. ESI-MS of the

90 assembly species exhibited an intense peak at m/z = 1027.51 with the isotopic distribution patterns separated by 0.33 Da. The peak

was assigned to [Zn$_6$(H**ZPT**)$_3$(**ZPT**)]$^{3+}$ species, indicating the successful assembly of a Zn$_6$L$_4$ molecular octahedron in solution (Fig. 3). Upon the addition of RDX, ESI−MS exhibited a new peak at *m/z* = 1101.52 with the isotopic distribution patterns separated by 0.33 Da. The peak is assignable to [Zn$_6$(H**ZPT**)$_3$(**ZPT**)⊃RDX]$^{3+}$ species through the comparison of this peak with the simulation results obtained on the basis of natural isotopic abundances. These results also demonstrated the formation of 1:1 host-guest complex, providing the possibility to interact with RDX in the cavity to prompt the formation of luminescent active species efficiently.
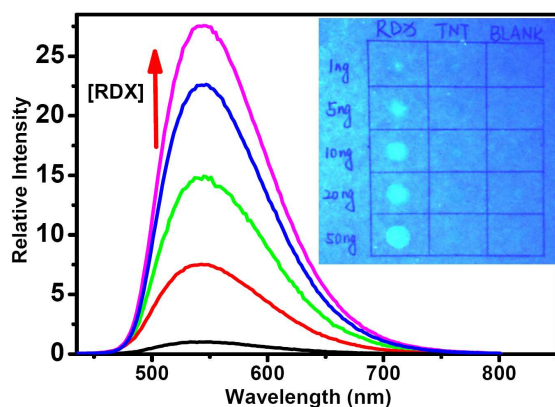
Fig. 4 The time-dependent fluorescence growth of Zn–**ZPT** (10 μM) in DMF solution upon addition of the RDX (1 μM) after irradiation with 310 nm light. Spectra were recorded at time intervals of 1 min. Excited at 415 nm. Insert exhibits visual fluorescence detection of RDX.

Zn–**ZPT** exhibited clear ligand-based charge-transfer bands (at about 300 and 415 nm) in a DMF solution (10 μM). The addition of RDX and irradiation (310 nm) caused a significant decrease in the absorbance intensity at 415 nm and clear increase at 330 nm. The presence of sharp isosbestic points at 315 and 345 nm indicates that only the reduction and oxidization state of NADH analogue coexist in equilibrium. When excited at 415 nm, Zn–**ZPT** (10 μM) in DMF exhibited a weak emission band centered on 545 nm. The addition of the RDX (1 μM) caused a *ca* 27 fold luminescent enhancement after a 5 min irradiation with 310 nm light (Fig. 4). The competition experiments showed that the fluorescence responses of RDX (1 μM) were unaffected in the presence of other explosives (10 μM). The results showed that the two compounds with different metal centres have similar fluorescence enhancement, which should derive from the formation of NAD$^+$ analogue.

Under optimized conditions, with the concentration of Zn–**ZPT** fixed at 5 μM, the fluorescence intensity of the Zn–**ZPT** solution is nearly proportional to the RDX concentration, and the addition of 1 ppb RDX causes about 20 % fluorescent enhancement within 5 min. The detection limit of 1 ppb represents the most sensitive chemosensor for RDX in solution. The more sensitive comparing to the mass spectrometric detection[21,22] suggested the opportunity for the application in the field of rapid detection of trace amount of explosives.

In order to detect explosive RDX in real world applications, the visual detection study of RDX was performed by preparing substrates spotted with Zn–**ZPT** and explosive RDX solution using DMF/acetonitrile as the solvent. The mixed solutions of Zn–**ZPT** (5 μM) and the desired RDX concentration were spotted onto filter paper with low background fluorescence using a glass microsyringe. A solvent blank was spotted next to each explosive. After a 1 min irradiation with 310 nm light, while RDX shows turn-on fluorescence detection as low as 1 ng, other explosives do not show any turn-on fluorescence even for spot loadings as high as 50 ng.

Notes and references

State Key Laboratory of Fine Chemicals, Dalian University of Technology Dalian, 116012, China. E-mail: cyduan@dlut.edu.cn

1. J. I. Steinfeld and J. Wormhoudt, *Annu. Rev. Phys. Chem.*, 1998, **49**, 203.
2. KD. Smith, BR. McCord, WA. McCrehan, K. Mount and WF. Rowe, *J. Forensic Sci.*, 1999, **44**, 789.
3. AM. Rouhi, *Chem Eng News*, 1997, **75**, 14.
4. S. J. Toal and W. C. Trogler, *J. Mater. Chem.*, 2006, **16**, 2871; J-S. Yang and T. M. Swager, *J. Am. Chem. Soc.*, 1998, **120**, 5321.
5. H. Sohn, M. J. Sailor, D. Magde and W. C. Trogler, *J. Am. Chem. Soc.*, 2003, **125**, 3821; S. J. Toal, D. Magde and W. C. Trogler, *Chem. Commun.* 2005, **43**, 5465.
6. J. Wang, R. K. Bhada, J. Lu and D. MacDonald, Anal. Chim. Acta, 1998, 361, 85; S. Hrapovic, E. Majid, Y. Liu, K. Male and J. H. T. Luong, *Anal. Chem.*, 2006, **78**, 5504.
7. H.-X. Zhang, A.-M. Cao, J.-S. Hu, L.-J. Wan and S.-T. Lee, *Anal. Chem.*, 2006, **78**, 1967; J. Wang, *Electroanalysis*, 2007, **19**, 415.
8. T. L. Andrew and T. M. Swager, *J. Am. Chem. Soc.*, 2007, **129**, 7254.
9. R. Freeman and I. Willner, *Nano Lett.*, 2009, **9**, 322.
10. M. Yoshizawa, J. K. Klosterman and M. Fujita, *Angew. Chem., Int. Ed.*, 2009, **48**, 3418.
11. L. Cronin, *Angew. Chem., Int. Ed.*, 2006, **45**, 3576.
12. A. Lützen, *Angew. Chem., Int. Ed.*, 2005, **44**, 1000.
13. M. D. Pluth, R. G. Bergman and K. N. Raymond, *Acc. Chem. Res.*, 2009, **42**, 1650.
14. J. Hamacek, G. Bernardinelli and Y. Filinchuk, *Eur. J. Inorg. Chem.*, 2008, 3419.
15. D. M. Vriezema, M. C. Aragonès, J. A. A. W. Elemans, J. J. L. M. Cornelissen, A. E. Rowan and R. J. M. Nolte, *Chem. Rev.*, 2005, **105**, 1445; M. Yoshizawa, J. K. Klosterman and M. Fujita, *Angew. Chem., Int. Ed.*, 2009, **48**, 3418.
16. Q. Chen, K. Gao, Y. Duan, Z. Ye, L. Shi, Y. Yang and Y. Zhou, *J. Am. Chem. Soc.,* 2012, **134**, 2442.
17. Crystal data: Ce–**ZBS** Ce$_4$C$_{170}$H$_{143}$N$_{29}$O$_{30}$: Ce$_4$(C$_{41}$H$_{30}$N$_7$O$_6$)$_4$·C$_3$H$_7$NO·3CH$_3$OH·2H$_2$O], M = 3632.61, Tetragonal, space group P4$_2$/n, black block, *a* = 18.598(3) Å, *c* = 31.814(6) Å, *V* = 11004(3) Å^3, *Z* = 2, Dc = 1.096 g cm^{-3}, μ(Mo-K$_α$) = 0.872 mm^{-1}, T = 180(2) K. 9689 unique reflections [R$_{int}$ = 0.0751]. Final R$_1$ [with I > 2σ(I)] = 0.0710, wR2 (all data) = 0.2566. CCDC number 972499.
18. A. M. Stadler and J. Harrowfield, *Inorg. Chim. Acta*, 2009, **362**, 4298.
19. I. K. Biernacka, A. Bartecki and K. Kurzak, *Polyhedron*, 2003, **22**, 997.
20. C. He, Z. Lin, Z. He, C. Duan, C. Xu, Z. Wang and C. Yan, *Angew. Chem. Int. Ed.*, 2008, **47**, 877.
21. R. Mu, H. Shi, Y. Yuan, A. Karnjanapiboonwong, J. G. Burken and Y. Ma, *Anal. Chem.*, 2012, **84**, 3427.
22. L. Ma, B. Xin and Y. Chen, *Analyst,* 2012, **137**, 1730.